Published in final edited form as:

Semin Ultrasound CT MR. 2018 December ; 39(6): 570–586. doi:10.1053/j.sult.2018.09.003.

Imaging-Based Approach to Extradural Infections of the Spine

Jason F. Talbott, MD, PhD[1,2], **Vinil N. Shah, MD**[2], **Alina Uzelac, DO**[1,2], **Jared Narvid, MD**[1,2], **Rebecca A. Dumont, MD**[2], **Cynthia T. Chin, MD**[2], and **David M. Wilson, MD, PhD**[2]

[1]Department of Radiology and Biomedical Imaging, Zuckerberg San Francisco General Hospital, San Francisco

[2]Department of Radiology and Biomedical Imaging, University of California, San Francisco

Keywords

MRI; spondylodiscitis; infection; diffusion weighted imaging; vertebral discitis-osteomyelitis

Extradural infections of the spine are increasing in frequency in the United States and around the world[12]. Timely and accurate diagnosis of spinal infection is essential, as it leads to improved outcomes and can be lifesaving. Because the clinical signs and symptoms of patients with spinal infection are often nonspecific, imaging plays a critical role in confirming a suspected diagnosis. This article will focus on the characteristic imaging features of extradural spinal infections with particular emphasis on findings seen with MRI. Specific imaging patterns that can be helpful for diagnosing spinal infection will be emphasized. Imaging features suggestive of common mimics of spinal infections will also be reviewed. Finally, the indications for image-guided tissue sampling will be reviewed.

EPIDEMIOLOGY OF SPINE INFECTION

Nearly all extradural spinal infections are caused by bacterial or fungal pathogens[3–5]. Bacterial spondylodiscitis is much more common than fungal[4]. Updated incidence and prevalence data for pyogenic vertebral osteomyelitis in the United States is lacking. Historically, the incidence of spondylodiscitis is reported as 1 case per 250,000 people in the population, accounting for 3%−5% of all cases of osteomyelitis[6]. The incidence, however, is rising due to a number of factors including improved diagnostic capabilities, increased intravenous drug use, an increase in healthcare-associated infections, increased spinal surgery, and increased number of susceptible populations, namely the immunosuppressed and elderly[27–10] A retrospective study from the United Kingdom found a 150% increase in spontaneous discitis-osteomyelitis (DOM) during the period between 2008 and 2011 compared with incidence data from 1995–1999[11]. There is a sex disparity with a male to female ratio of 1.5 to 2:1 for vertebral osteomyelitis[12].

Corresponding author: Jason F. Talbott (Jason.talbott@ucsf.edu), 415-206-2942 (Phone), 415-206-4004 (Fax), Zuckerberg San Francisco General Hospital, Department of Radiology, 1001 Potrero Avenue, Room 1X57C, San Francisco, CA 94110.

Among bacterial spine infections, *Staphylococcus aureus* (*S. aureus*) is the most common pathogen accounting for approximately half of pyogenic infections[13–15]. Gram-negative bacteria and streptococci pathogens account for most of the remaining cases. Streptococci and enterococci are more strongly associated with infective endocarditis as the primary source of infection[2]. Non-pyogenic, granulomatous extradural infections of the spine include tuberculosis, fungal, and rarely the Echinococcal parasite. Tuberculous spinal infections are primarily endemic to developing nations; however, such infections remain a significant problem in developed countries as well, including the United States. A recent epidemiologic study based upon The Nationwide Inpatient Sample database from 2002 to 2011 revealed a small absolute reduction in spinal TB cases in the US over this time period, with an average of 279 cases per year[16].

Although precise incidence data is not available, disseminated fungal infections of the extradural spine are rare and primarily seen in immunocompromised individuals, with Candida and Aspergillus species as the most commonly reported agents[17]. Fungal spondylodiscitis comprises approximately 1% of cases[2].

PATHOPHYSIOLOGY

Insight to the pathophysiologic mechanisms of infectious spread to the spine can inform interpretation of the imaging findings. The most common route of spinal contamination is via hematogenous spread of infection, which is most commonly arterial, but can also be venous. A rich arterial network supplies the vertebral body with proliferation of arterioles most densely at the endplates, particularly the ventral subchondral zones (fig 1). As a result, infectious arterial emboli often initially seed this region with ultimate direct extension of infection to the intervertebral disc and adjacent endplate[18, 19]. The most common primary source is urinary tract infection, followed by skin and the upper respiratory tract[4, 20].

In neonates and young children, numerous channels remain patent across the cartilaginous vertebral endplates (fig 1). These channels are traversed by small end arterioles resulting in primary seeding at the adjacent disc, rendering young children more susceptible to primary discitis preceding development of osteomyelitis[21]. In older children and adults, these channels close, with an associated reduced incidence of primary discitis[21] (fig 1). There is also an extensive epidural valveless venous plexus of the spine which serves as a potential route for venous hematogenous spread for infection, particularly in the setting of primary infections of the pelvic organs including the urinary bladder and female reproductive organs[22].

Non-hematogenous routes of spinal contamination include direct, contiguous spread to the spine from adjacent organs such as para-pneumonic empyema and retroperitoneal abscess. Close attention to adjacent spinal structures on spine imaging can help identify the primary source of infection in these cases. Iatrogenic inoculation with contaminated instrumentation or injectate highlights the importance of assessing procedural history in a patient with suspected spinal infection. A recent outbreak of 749 spinal fungal infections related to contaminated steroid injections in the United States is an extreme example of this route of

spread[23]. Penetrating trauma and open surgical procedures similarly present an opportunity for direct inoculation of infection[3, 4].

IMAGING SPONDYLODISCITIS

Magnetic resonance imaging (MRI) is the modality of choice for initial diagnosis of spinal infections, with reported sensitivity of 96% and specificity of 93% for an accuracy of 94%[2, 4]. Conventional T1-weighted (T1w) and T2w sequences are necessary to show characteristic fluid signal (T1 hypointensity, T2 hyperintensity) within the intervertebral disc, vertebral endplate and adjacent marrow space related to DOM (fig 2, 3). Application of fat suppression techniques with T2w sequences enhances sensitivity to spinal and para-spinous edema. When gadolinium is not contraindicated, T1-post contrast imaging is important for identifying infection-related enhancement in the spine. As with T2w imaging, application of fat suppression for T1 postcontrast sequences enhances sensitivity to pathologic enhancement. Increasingly, sagittal diffusion weighted imaging (DWI) is routinely included in cases of suspected spinal infection. DWI is particularly useful in characterizing the nature of spinal fluid collections and differentiating spondylodiscitis from reactive bone marrow edema observed in bland degenerative disc disease[24].

As a complementary study, and in some cases, as a primary modality when MRI cannot be performed due to patient intolerance or other contraindication, nuclear medicine studies may provide useful diagnostic information[25]. Bone scintigraphy with the radionuclide technetium-99m diphosphonate is often used for initial screening, however false negative results are common, associated paraspinous soft tissue infections are poorly visualized, and radionuclide uptake may persist long after an infection has resolved[25, 26]. Gallium-67 citrate (^{67}Ga) supplements conventional bone scintigraphy and is often used in combination with a bone scan to improve sensitivity and with single photon emission computed tomography (SPECT) technique to enhance radionuclide uptake localization[25, 27]. Soft-tissue infection accompanying DOM is more reliably observed with ^{67}Ga and more sensitive detection of early infection has been reported[25, 26]. Due to its non-specificity, WBC imaging is not recommended for evaluation of spine infection[25]. Combined positron emission tomography (PET) and CT (PET/CT) imaging with 2-[^{18}F]-fluoro-2-deoxy-D-glucose (FDG) has been shown to be superior to ^{67}Ga and bone scintigraphy for diagnosing spinal infections[28–31]. For detection of early or low-grade DOM, FDG-PET may be superior to MRI[30–32].

CT may also be performed as a complimentary imaging study in cases of suspected spinal infection due to its superior role in delineating bony abnormalities including endplate and vertebral body erosion and for assessing bone quality for pre-surgical evaluation. Identification of paraspinous soft tissue calcification is also useful as a common manifestation of advanced turberculous spondylitis[33]. Due to its low sensitivity, plain radiography has little role in modern workup of spinal infection.

PYOGENIC DISCITIS-OSTEOMYELITIS (DOM)

Pyogenic DOM is the most common infection of the spine and familiarity with its characteristic imaging features is critical for accurate diagnosis. Clinical presentation is

often subtle with insidious onset of nonspecific symptoms including back pain, malaise, weight loss, and fever. There are no specific serum biomarkers and leukocytosis is commonly absent[3]. Although nonspecific, elevations in erythrocyte sedimentation rate (ESR) and C-reactive protein (CRP) are frequently observed[3]. As a result, imaging is paramount in confirming a suspected clinical diagnosis.

Lumbar spinal levels are most frequently involved, followed by thoracic and cervical[520]. Infection characteristically begins in the metaphyseal region of the vertebral body with direct spread to the intervertebral disk and adjacent vertebral endplate. Infection of marrow and endplate manifests in the earliest stages of infection as T1 hypointense, T2 hyperintense fluid signal of the involved bone and disc, with associated confluent bone enhancement[5, 20, 34] (fig 2). In more advanced stages of infection, endplate erosions and vertebral body destruction may be observed (fig 3). The disc space is typically involved very early with pyogenic spine infection and similar to vertebral marrow space, the disc exhibits T2 hyperintense fluid signal with height loss, but more variable patterns of enhancement[5,20, 34]. Enhancement distribution coincides with regions of spinal edema, except in regions of frank necrosis or abscess formation, such as centrally within an involved disc (fig 2–4). In areas of abscess or necrosis, enhancement is irregular and peripheral and absent centrally.

Extension of infection beyond the discovertebral complex is a common finding with pyogenic DOM, especially in the later stages of infection (fig 3–5). Evaluation for paraspinous and epidural spread of infection is important both for management decisions and for confirmation of diagnosis. Spinal epidural abscess (SEA) formation is suspected when a focal fluid collection with peripheral enhancement and central T2 hyperintensity is present in the epidural space (fig 6). Similar to imaging features of purulent abscess in other parts of the body, diffusion-weighted imaging (DWI) may reveal uniform hyperintense signal with corresponding reduced apparent diffusion coefficient (ADC) values overlapping regions of nonenhancing, T2-hyperintense purulent collection (fig 6) [3, 5, 20]. In some cases, more solidly enhancing epidural soft tissue thickening is encountered and often referred to as epidural “phlegmon”. Phlegmonous epidural infection may precede the development of frank SEA and is less amenable to surgical drainage, (fig 7).

Morbidity and mortality related to SEA is high, not only because of the risk of subdural and intrathecal spread, but also due to direct spinal cord and/or cauda equina compression[3, 5, 20] (figs 3–8). Patients may rapidly progress with pyramidal motor, sensory and autonomic deficits necessitating rapid diagnosis and treatment to prevent permanent disability. SEA rarely occurs in isolation. In more than 80% of cases, there will be associated DOM, septic facet joint infection, or adjacent paraspinous/retroperitoneal infection, which should be identified on imaging as the primary source of the spinal infection so that appropriate and directed treatment can be initiated[3]. *S. aureus* is the culprit pathogen in nearly 70% of SEA cases[3]. Paraspinal soft tissue involvement is confirmed when abnormal enhancement and edema or frank abscess formation involving the paraspinous muscles and intervening fat planes is observed (figs 4,5). T1, T2, enhancement, and DWI features of paraspinous abscess and phlegmon are similar to those described for epidural infection reviewed above[3, 5, 20, 35].

Several conventional MR imaging features observed in DOM have been evaluated for their diagnostic sensitivity and specificity[35]. Ledbetter and colleagues recently evaluated the diagnostic accuracy for many of these features in a retrospective case-control study including 51 patients with a confirmed diagnosis of DOM[36]. Among non-contrast imaging findings, psoas muscle T2 hyperintensity (referred to as the 'psoas' sign) had the highest sensitivity (92%) and specificity (92%) for diagnosing lumbar spondylodiscitis[36] (fig 9). Other findings with high sensitivity and specificity include psoas muscle enhancement, vertebral body T2 hyperintensity, and presence of epidural phlegmon[36]. Findings with lower specificity include intervertebral disc T2 hyperintensity (76%) and a rim pattern of disc enhancement (31%)[37].

Over the past decade, the added value of DWI for diagnosing spinal infection has been demonstrated[5, 24, 38]. Degenerative disc desiccation with fibrovascular reactive endplate and vertebral body marrow edema, referred to as Modic type 1 changes, mimics many of the imaging features of DOM as will be discussed in more detail in a subsequent section related to spine infection mimics[39]. Patel and colleagues reported a characteristic pattern on sagittal DWI sequence in Modic 1 pathology consisting of paired, leading edge DWI hyperintense bands emanating from an intervertebral disc[24] (fig 10). When this finding, referred to as the 'claw' sign, was definitively observed, virtually all patients (38/39, 97%) were infection free. In cases of confirmed DOM, the claw sign was absent and more diffuse DWI hyperintensity throughout the involved vertebral bodies was observed (fig 11). A detailed description of ADC values is not included in the original description of the claw sign due to poor signal to noise of the diffusion data[24]. In our experience, the vertebral marrow DWI hyperintensity comprising the claw sign is usually not correlated with reduced ADC values, but rather relates to T2-shine through (fig 10).

Dumont and colleagues more recently evaluated the diagnostic validity of quantitative ADC measures in cases of suspected spinal infection[38]. In that study, which included 38 patients, those patients with positive microbiological sampling had significantly lower ADC values in interrogated regions that were suspicious for infection on imaging[38]. Establishing an ADC threshold value of 1,250 mm^2/s yielded a sensitivity of 66% and specificity of 88% for diagnosing spine infection.

SPECIAL CONSIDERATIONS

Post-treatment surveillance

In addition to helping with initial diagnosis, MRI is often performed to monitor response to antibiotic therapy for DOM. The diagnostic utility for this application however, is not well documented. Available data suggests that post-treatment MRI evaluation should focus on soft tissue findings[40–43]. Kowalski and colleagues examined osseous and soft tissue findings in 33 patients with baseline and follow-up MRI obtained 4–8 weeks after treatment[43]. While bone marrow and disc edema, enhancement and vertebral height loss may progress or remain equivocal compared with baseline, interval decrease in epidural enhancement, epidural and paraspinous abscess, and epidural enhancement consistently improve on follow-up (fig 12). No single imaging feature, however, was significantly associated with

successful treatment[43]. Larger prospective trials are needed to identify definitively the best biomarkers of successful treatment.

In cases of unambiguous progression of infection, one potential consideration for treatment failure is polymicrobial infection (fig 13). Polymicrobial infections are associated with older age and higher mortality[44]. However, incidence data and clinical significance of polymicrobial spine infections are sparse. In a cohort of patients requiring spinal instrumentation for vertebral DOM, only 2% (2/94) of cases were associated with polymicrobial infection[45]. However, in a retrospective review of spontaneous DOM in the United Kingdom, Sur and colleagues identified multiple organisms from spine culture specimens in up to 11% of cases (6/55)[11]. Therefore, in cases of treatment failure, polymicrobial infection should be considered. Further study of the clinical significance of polymicrobial infection is warranted[44].

Post-operative spine infection

Imaging for new or residual infection in the postoperative setting presents unique challenges related to postoperative findings that can mimic infection, such as seroma formation and enhancing granulation tissue[46]. DOM as a complication of spine disc surgery is fortunately a relatively infrequent occurrence[3, 47]. *S. aureus* accounts for 45% of surgical site infections (SSI)[47]. A recent review of more than 1700 patients undergoing instrumented spinal fusion identified SSIs in 3% (58/1764) of patients who were followed for up to 1 year after surgery, with polymicrobial infections in 61% of these cases[48]. These results are consistent with prior data published by Abdul-Jabbar and colleagues who evaluated SSIs incidence and risk factors for more than 7000 spine surgery patients[47].

Normal post-operative findings on MRI may mimic those of acute infection. For example, intra-discal contrast enhancement and T2w signal hyperintensity on post-operative MRI may persist for weeks following discectomy. However, the absence of new endplate and subchondral marrow edema or enhancing paravertebral soft tissues may help exclude a postoperative DOM[49]. DWI can aid in characterizing the nature of postoperative collections[50]. Ubiquitous postoperative seromas have elevated ADC values similar to simple fluid compared with confluent hindered diffusion that characterizes pyogenic abscess.

Another potential complicating factor of imaging the postoperative spine with MRI relates to susceptibility artifact from hardware[3]. DWI is particularly sensitive to susceptibility artifact, which can limit its application. Spinal instrumentation also introduces significant artifact for conventional T1w and T2w sequences. In the setting of instrumentation, steps should be taken to minimize susceptibility artifact from hardware and imaging at 1.5 Tesla is preferred over 3 Tesla[50]. Hardware interference with fat suppression can complicate interpretation of T2 hyperintensity and enhancement of tissues adjacent to the hardware; therefore inclusion of non fat-suppressed sequences may be helpful for problem solving.

Septic facet joint

Although there is little available epidemiological data and incidence is likely underreported, based on published case reports, primary spine infections of the facet joints are relatively rare compared with DOM[20,51,52]. In a single institution review, septic facet arthritis

accounted for 4% (6/140) of pyogenic spinal infections[52]. 90% of cases involved the lumbar spine[51]. As with DOM, predisposing factors include immunosuppression, DM, and pre-existing chronic illness[53]. *S. Aureus* is the most common causative organism. Iatrogenic causes related to corticosteroid injections have been reported. Therefore, in suspected cases, it is important to obtain history of any prior invasive spinal prodedures[54]. Septic facet arthritis is treated with long-term intravenous antibiotics. For complicated cases with abscess formation, percutaneous or surgical drainage may be required.

As with extraspinal joint infections, bone marrow edema and enhancement centered about the joint are present with septic facet arthritis[20, 55] (figs 14,15). Joint space widening and intra-articular fluid may also be observed (fig 15). With more advanced infections, erosive changes of the articular surface and subchondral bone with synovitis and peri-synovial inflammation are common[56] (figs 14, 15). Abscess formation may occur within or around the affected joint (fig 14, 15). Due to potential communication between a lumbar facet joint and the posterior ligamentous complex via the retrodural space of Okada, direct extension of facet infection to interspinous bursa and contralateral facet joint may be observed[57–59]. As for DOM, imaging features of septic facet arthropathy overlap with non-infectious degenerative and inflammatory spondyloarthropathies[3760]. Blood and infected tissue sample cultures may therefore be needed for confirmation when imaging and clinical findings are indeterminate. Primary spinal infections of the posterior elements other than the facet joints, including costotransverse and costovertebral joints, have been rarely described in the literature[61] (fig 16).

ATYPICAL SPINAL INFECTIONS

Tuberculous Spondylitis (TS)

TS is a granulomatous bacterial infection of the spine caused by *Mycobacterium tuberculosis*, a gram positive acid fast bacillus. The thoracolumbar spine is most commonly involved with TS, with seeding often from a quiescent pulmonary focus[343562]. Compared with pyogenic DOM, TS tends to have a more indolent clinical course with presenting symptoms comprised of back pain and kyphotic deformity preceded by systemic symptoms of weight loss, fever, and malaise[353435]. The TS-related spine deformity, popularly referred to as Pott's spine, traces back to the original description of TS by Sir Percival Pott in his monograph in 1779[63].

Many of the imaging features of TS overlap with pyogenic DOM and caution should be used in over-reliance on imaging for making a specific microbiological diagnosis. Nevertheless, suggestive imaging findings have been described. Typically, intervertebral disc involvement is relatively mild with TS compared to pyogenic DOM due to lack of proteolytic enzymes required for disc invasion[353562] (fig 17). Predilection for anterior column vertebral involvement can lead to anterior vertebral collapse and associated kyphosis, referred to as gibbous deformity (fig 13). Intraosseous vertebral abscess with central caseating necrosis and rim enhancement pattern should clue the diagnostician to a diagnosis of TS. Compared with pyogenic DOM, TS is more likely to simultaneously involve both the anterior and posterior elements of the spine[364]. Contiguous paraspinous and epidural spread of infection is typical[33562] (fig 13, 17). The findings of anterior subligamentous extension and paraspinal

abscesses containing smooth walls and surrounding coarse calcifications can aid in suggesting a diagnosis of TS[33562]. The presence of multiple vertebral level involvement with intervening normal levels, so-called “skip” lesions, is also suggestive of TS over pyogenic DOM (fig 13)[362].

Fungal Spondylitis (FS)

Disseminated fungal infection with spondylitis is primarily a disease of the immunocompromised. Candida and Aspergillus species are the most frequent offending pathogens[33565]. FS has a predilection for lumbar spine involvement[66]. As with TS, fungal infection often presents with skip lesions, subligamentous spread, and widely disseminated paraspinous soft tissue infection with abscesses[335] (fig 18). Intervertebral discs are typically spared with FS, including preservation of the normal T2 hypointense intranucler cleft and lack of characteristic T2 hyperintensity associated with pyogenic DOM[366]. The presence of any of these findings in an immunocompromised patient should raise the suspicion for FS.

Brucellar Spondylitis (BS)

Brucellosis is a highly contagious zoonosis caused by ingesting unpasteurized milk or undercooked meat from infected animals[67]. This gram negative bacillus is endemic to parts of the Mediterranean basin. When infection involves the spine, lower lumbar levels are predominantly involved, compared with thoracolumbar predominance of TS[68]. Subligamentous spread is uncommon, as is vertebral destruction and paraspinous abscess formation. Posterior elements are typically spared with BS[68].

SPINE INFECTION MIMICS

Many of the imaging features described for pyogenic DOM are nonspecific and may also be seen with non-infectious pathologies of the spine[69]. Some of the more frequently encountered differential diagnostic considerations are reviewed below.

Degenerative disc disease and traumatic cartilaginous nodes (Schmorl’s node)

The most commonly encountered mimic of DOM is degenerative disc disease. As described above, DWI findings and the presence of the psoas sign on T2-weighted sequences can help distinguish acute infection from Modic 1 changes associated with degenerative disc disease[2436] (figs 9, 10). In cases of suspected DOM, careful attention to attenuation characteristics of the affected intervertebral disc on CT should also be given as the presence of hypodense air within a disc (i.e. degenerative vacuum phenomenon) makes the diagnosis of active discitis less likely[37]. However, degenerative vacuum phenomenon does not exclude acute DOM and cases of acute DOM with co-existent vacuum phenomenon are described in the literature[69] (fig 19). Spinal infections related to gas producing organisms, such as *clostridium perfringens,* are exceedingly rare. A few published case reports describe extensive associated pneumorrhachis (air throughout the spinal canal) with gas-forming spinal infections, helping to distinguish from the much more common finding of degenerative disc vacuum phenomenon[70]. In a small retrospective study FDG-PET was evaluated to complement MRI for distinguishing bland degenerative disc disease from

DOM[32]. Compared with avid FDG uptake in DOM, non-infected Modic 1 degenerative changes were associated with absence of FDG uptake[32].

Given the overlapping imaging and clinical features, it has been suggested that Modic-1 degenerative disc disease is caused by low-grade chronic infection of the disc in some cases[71]. However, this remains a controversial hypothesis with contradictory evidence in the literature[72]. Associations between anaerobic bacterial infection of discs with *Propionibacterium acnes (P. acnes)* and Modic 1 changes on MRI have been reported recently[7173]. However, *P. acnes* is a ubiquitous skin flora and well-known contaminant of culture specimens[74]. When utilizing surgical techniques to minimize disc biopsy contamination, Rigal and colleagues found no association between subclinical infection and disc degeneration[75]. While the hypothesis that low grade infection may contribute to degenerative disc pathology is intriguing and could lead to potential new therapeutic options for discogenic low back pain, the literature on this topic remains mixed and further studies are needed to establish causation[76].

In addition to Modic 1 degenerative disc disease, acute traumatic cartilaginous nodes, or Schmorl's nodes, may present with nonspecific axial low back pain similar to DOM[77]. Defined as upward extrusion of disc material into the intramedullary space of an adjacent vertebral body, Schmorl's nodes may be associated with surrounding bone marrow edema and hyper-enhancement on MRI, mimicking the imaging appearance of acute DOM[6978]. Identification of a focal endplate defect with edema and enhancement centered about this defect in addition to lack of significant paraspinous or epidural abnormality are useful MR imaging findings to favor the diagnosis of acute cartilaginous Schmorl's node[69].

Dialysis-related spondyloarthropathy

Dialysis-related spondyloarthorpathy also has overlapping imaging and clinical features with infectious spondylodiscitis[7980]. Amyloid deposition in the disk and spinal ligaments results in diminished disc height and erosion of vertebral endplates, similar to infectious spondylodiscitis[79]. Unlike infectious edema, however, amyloid deposition accelerates T2 signal decay with resultant hypointense T2 signal in involved regions of disc, bone, and ligaments. Additional imaging findings more suggestive of dialysis-associated spondyloarthrapathy include well demarcated endplate errosions[81]. Biopsy may be necessary to confirm the diagnosis of dialysis-related spondyloarthropathy with positive amyloid staining.

Spinal neuroarthropathy (SNA)

SNA, sometimes referred to as Charcot spine, may also mimic many of the imaging features seen with pyogenic DOM (Fig 20)[37]. Spinal cord injury results in loss of deep sensation and proprioceptive input from the spine. A combination of neurotraumatic and neurovascular mechanisms after cord injury contribute to the pathophysiology of SNA with progressive destruction of the discovertebral complex and facet joints[37]. Thoracolumbar and lumbosacral levels are most commonly involved with bone fragmentation, erosion, sclerosis, and malalignment. Several helpful imaging findings have been described to help differentiate between SNA and DOM as recently reviewed by Ledbetter et al.[37] While

pyogenic DOM is typically centered at the endplates and intervertebral disc, SNA involves the entire intervertebral joint, including the bilateral facet joints[37]. Other findings more suggestive of SNA include presence of gas within the intervertebral disc[37], and prominent finding of bony sclerosis and peri-articular bony debris on CT[37] (fig 20).

Vertebral osteonecrosis

Vertebral osteonecrosis results from ischemic necrosis and nonunion fracture following vertebral body compression injury. With variable degrees of flexion and extension, increased separation of the nonunion vertebral fracture underlying the superior endplate contributes to vacuum phenomenon with accumulation of gas and transudative fluid[82]. While the necrotic changes of the vertebral body may mimic those of severe, erosive osteomyelitis, relative sparing of the intervertebral disc can help distinguish osteonecrosis from DOM. Further, the presence of an intra-vertebral wedge-shaped T2 hyperintensity on MRI and associated air cleft on CT (vacuum cleft sign), is pathonomonic for vertebral osteonecrosis, helping to exclude vertebral osteomyelitis[82] (fig 21).

Ankylosing spondylitis (AS)

Autofusion of the spine is a characteristic manifestation of ankylosing spondylitis (AS). As a result of altered spinal biomechanics and osteoporotic changes associated with AS, 3-column spinal stress fractures can occur with minimal inciting force[3769]. If diagnosis is delayed, a pseudoarthrosis, or abnormal motion across the fused spine, may develop at the fracture level with associated endplate bone erosion and subchondral sclerosis; radiographic features mimicking infectious DOM[37] (fig 22). Along with clinical context, CT and MRI may prove helpful in distinguishing AS-related pseudo-arthrosis from infectious DOM with visualization of a fracture line across the posterior elements and absent paraspinous or epidural phlegmon or abscess[69].

SPINE BIOPSY FOR INFECTION

When imaging and clinical findings suggest the diagnosis of spine infection but blood cultures are negative, current Infectious Diseases Society of America (IDSA) guidelines recommend direct biopsy of infected tissues with imaging guidance for confirmation[27]. Percutaneous biopsy may also be indicated when the diagnosis is known, but identification of a specific organism is desired to tailor antibiotic treatment.

The reported accuracy of percutaneous biopsy for spine infection is highly variable, in part related to heterogeneity between centers with respect to history of antibiotic therapy, number of specimens obtained, and experience level and technique of the performing radiologist[2]. In a recent meta-analysis including 33 studies between 1980 and 2016, McNamarra et al. found an average yield of 48% for diagnosis of DOM with image-guided biopsy (range of 31% to 91%)[83]. This compares with a yield of 76% for open surgical biopsy[83]. Importantly, a trend toward reduced yields in patients with prior antibiotic treatment was observed, although this reduction was not statistically significant[83]. Kim et al. utilized multivariate statistics to identify clinical and imaging factors predictive of biopsy positivity and identified a negative correlation with prior antibiotic therapy, which was statistically significant in patients with 4

or more days of prior antibiotic treatment[84]. Marschall and colleagues did not find a significant decrease in yield in a cohort of 92 patients with suspected DOM, 60 of which were started on empirical antibiotics prior to biopsy[85]. However, the authors note that patients with prior antibiotic therapy had more advanced infection, potentially confounding these results[85]. IDSA guidelines recommend holding antibiotic treatment prior to diagnostic aspiration in patients who are hemodynamically stable and without neurologic compromise[86]. Diagnostic yields may also be enhanced with collection of a core biopsy specimen for dedicated histologic analysis in addition to specimens for microbiology[8788]. Because paravertebral and intra-discal fluid collections are often sterile, inclusion of subchondral bone in core samples may also increase yield[87] (fig 23). At our institution, biopsies are performed with CT-guidance using coaxial technique via a transpedicular or para-pedicular approach with collection of multiple core specimens, including both disc and adjacent endplate (fig 23).

CONCLUSION

Timely and accurate diagnosis of extradural spine infections is highly dependent on imaging. MRI is the gold standard imaging modality for spinal infections with complementary roles in select cases for CT and nuclear medicine imaging, particularly ^{67}Ga/^{99m}Tc scintigraphy and FDG-PET. Familiarity with characteristic imaging features of DOM as well as other primary extradural sites of spinal infection is imperative for accurate diagnosis and for exclusion of potential non-infectious differential diagnostic considerations. In addition to diagnosing the primary site of infection for timely antibiotic therapy, imaging facilitates identification of secondary spread of infection and associated complications, such as spinal cord or cauda equina compression, guiding emergent intervention and significantly reducing morbidity and mortality. In cases where diagnosis is unclear or determination of the inciting pathogen is needed to narrow the spectrum of antibiotics, percutaneous image-guided tissue sampling may obviate the need for more invasive open surgical biopsy.

REFERENCES

1. Jensen AG, Espersen F, Skinhoj P, et al. Increasing frequency of vertebral osteomyelitis following Staphylococcus aureus bacteraemia in Denmark 1980–1990. The Journal of infection 1997;34(2): 113–8. [PubMed: 9138133]
2. Gouliouris T, Aliyu SH, Brown NM. Spondylodiscitis: update on diagnosis and management. The Journal of antimicrobial chemotherapy 2010;65 Suppl 3:iii11–24. [PubMed: 20876624]
3. DeSanto J, Ross JS. Spine infection/inflammation. Radiologic clinics of North America 2011;49(1): 105–27. [PubMed: 21111132]
4. Arbelaez A, Restrepo F, Castillo M. Spinal infections: clinical and imaging features. Topics in magnetic resonance imaging : TMRI 2014;23(5):303–14. [PubMed: 25296275]
5. Go JL, Rothman S, Prosper A, et al. Spine infections. Neuroimaging clinics of North America 2012;22(4):755–72. [PubMed: 23122265]
6. Sobottke R, Seifert H, Fatkenheuer G, et al. Current diagnosis and treatment of spondylodiscitis. Deutsches Arzteblatt international 2008;105(10):181–7. [PubMed: 19629222]
7. Musher DM, Thorsteinsson SB, Minuth JN, et al. Vertebral osteomyelitis. Still a diagnostic pitfall. Archives of internal medicine 1976;136(1):105–10. [PubMed: 1247327]
8. Torda AJ, Gottlieb T, Bradbury R. Pyogenic vertebral osteomyelitis: analysis of 20 cases and review. Clinical infectious diseases : an official publication of the Infectious Diseases Society of America 1995;20(2):320–8. [PubMed: 7742437]

9. Deyo RA, Nachemson A, Mirza SK. Spinal-fusion surgery - the case for restraint. The New England journal of medicine 2004;350(7):722–6. [PubMed: 14960750]
10. Carragee EJ. Pyogenic vertebral osteomyelitis. The Journal of bone and joint surgery American volume 1997;79(6):874–80. [PubMed: 9199385]
11. Sur A, Tsang K, Brown M, et al. Management of adult spontaneous spondylodiscitis and its rising incidence. Annals of the Royal College of Surgeons of England 2015;97(6):451–5. [PubMed: 26274746]
12. Mylona E, Samarkos M, Kakalou E, et al. Pyogenic vertebral osteomyelitis: a systematic review of clinical characteristics. Seminars in arthritis and rheumatism 2009;39(1):10–7. [PubMed: 18550153]
13. Hadjipavlou AG, Mader JT, Necessary JT, et al. Hematogenous pyogenic spinal infections and their surgical management. Spine 2000;25(13):1668–79. [PubMed: 10870142]
14. Legrand E, Flipo RM, Guggenbuhl P, et al. Management of nontuberculous infectious discitis. treatments used in 110 patients admitted to 12 teaching hospitals in France. Joint, bone, spine : revue du rhumatisme 2001;68(6):504–9.
15. Turunc T, Demiroglu YZ, Uncu H, et al. A comparative analysis of tuberculous, brucellar and pyogenic spontaneous spondylodiscitis patients. The Journal of infection 2007;55(2):158–63. [PubMed: 17559939]
16. De la Garza Ramos R, Goodwin CR, Abu-Bonsrah N, et al. The epidemiology of spinal tuberculosis in the United States: an analysis of 2002–2011 data. Journal of neurosurgery Spine 2017;26(4):507–12. [PubMed: 27982765]
17. Thurnher MM, Olatunji RB. Infections of the spine and spinal cord. Handbook of clinical neurology 2016;136:717–31. [PubMed: 27430438]
18. Ratcliffe JF. An evaluation of the intra-osseous arterial anastomoses in the human vertebral body at different ages. A microarteriographic study. Journal of anatomy 1982;134(Pt 2):373–82. [PubMed: 7076561]
19. Wiley AM, Trueta J. The vascular anatomy of the spine and its relationship to pyogenic vertebral osteomyelitis. The Journal of bone and joint surgery British volume 1959;41-B:796–809. [PubMed: 13855377]
20. Torres C, Zakhari N. Imaging of Spine Infection. Seminars in roentgenology 2017;52(1):17–26. [PubMed: 28434499]
21. Ratcliffe JF. Anatomic basis for the pathogenesis and radiologic features of vertebral osteomyelitis and its differentiation from childhood discitis. A microarteriographic investigation. Acta radiologica: diagnosis 1985;26(2):137–43. [PubMed: 3993417]
22. Tyrrell PN, Cassar-Pullicino VN, McCall IW. Spinal infection. European radiology 1999;9(6): 1066–77. [PubMed: 10415237]
23. Kauffman CA, Pappas PG, Patterson TF. Fungal infections associated with contaminated methylprednisolone injections. The New England journal of medicine 2013;368(26):2495–500. [PubMed: 23083312]
24. Patel KB, Poplawski MM, Pawha PS, et al. Diffusion-weighted MRI “claw sign” improves differentiation of infectious from degenerative modic type 1 signal changes of the spine. AJNR American journal of neuroradiology 2014;35(8):1647–52. [PubMed: 24742801]
25. Love C, Palestro CJ. Nuclear medicine imaging of bone infections. Clinical radiology 2016;71(7): 632–46. [PubMed: 26897336]
26. Love C, Patel M, Lonner BS, et al. Diagnosing spinal osteomyelitis: a comparison of bone and Ga-67 scintigraphy and magnetic resonance imaging. Clinical nuclear medicine 2000;25(12):963–77. [PubMed: 11129162]
27. Berbari EF, Kanj SS, Kowalski TJ, et al. 2015 Infectious Diseases Society of America (IDSA) Clinical Practice Guidelines for the Diagnosis and Treatment of Native Vertebral Osteomyelitis in Adults. Clinical infectious diseases : an official publication of the Infectious Diseases Society of America 2015;61(6):e26–46. [PubMed: 26229122]
28. Fuster D, Sola O, Soriano A, et al. A prospective study comparing whole-body FDG PET/CT to combined planar bone scan with 67Ga SPECT/CT in the Diagnosis of Spondylodiskitis. Clinical nuclear medicine 2012;37(9):827–32. [PubMed: 22889769]

29. Guhlmann A, Brecht-Krauss D, Suger G, et al. Fluorine-18-FDG PET and technetium-99m antigranulocyte antibody scintigraphy in chronic osteomyelitis. Journal of nuclear medicine : official publication, Society of Nuclear Medicine 1998;39(12):2145–52.
30. Schmitz A, Risse JH, Grunwald F, et al. Fluorine-18 fluorodeoxyglucose positron emission tomography findings in spondylodiscitis: preliminary results. European spine journal : official publication of the European Spine Society, the European Spinal Deformity Society, and the European Section of the Cervical Spine Research Society 2001;10(6):534–9.
31. Gratz S, Dorner J, Fischer U, et al. 18F-FDG hybrid PET in patients with suspected spondylitis. European journal of nuclear medicine and molecular imaging 2002;29(4):516–24. [PubMed: 11914890]
32. Stumpe KD, Zanetti M, Weishaupt D, et al. FDG positron emission tomography for differentiation of degenerative and infectious endplate abnormalities in the lumbar spine detected on MR imaging. AJR American journal of roentgenology 2002;179(5):1151–7. [PubMed: 12388490]
33. Bernaerts A, Vanhoenacker FM, Parizel PM, et al. Tuberculosis of the central nervous system: overview of neuroradiological findings. European radiology 2003;13(8):1876–90. [PubMed: 12942288]
34. Diehn FE. Imaging of spine infection. Radiologic clinics of North America 2012;50(4):777–98. [PubMed: 22643395]
35. Prodi E, Grassi R, Iacobellis F, et al. Imaging in Spondylodiskitis. Magnetic resonance imaging clinics of North America 2016;24(3):581–600. [PubMed: 27417402]
36. Ledbetter LN, Salzman KL, Shah LM. Imaging Psoas Sign in Lumbar Spinal Infections: Evaluation of Diagnostic Accuracy and Comparison with Established Imaging Characteristics. AJNR American journal of neuroradiology 2016;37(4):736–41. [PubMed: 26585257]
37. Ledbetter LN, Salzman KL, Sanders RK, et al. Spinal Neuroarthropathy: Pathophysiology, Clinical and Imaging Features, and Differential Diagnosis. Radiographics : a review publication of the Radiological Society of North America, Inc 2016;36(3):783–99.
38. Dumont RA, Keen NN, Bloomer CW, et al. Clinical Utility of Diffusion-Weighted Imaging in Spinal Infections. Clinical neuroradiology 2018.
39. Modic MT, Steinberg PM, Ross JS, et al. Degenerative disk disease: assessment of changes in vertebral body marrow with MR imaging. Radiology 1988;166(1 Pt 1):193–9. [PubMed: 3336678]
40. Carragee EJ. The clinical use of magnetic resonance imaging in pyogenic vertebral osteomyelitis. Spine 1997;22(7):780–5. [PubMed: 9106320]
41. Gillams AR, Chaddha B, Carter AP. MR appearances of the temporal evolution and resolution of infectious spondylitis. AJR American journal of roentgenology 1996;166(4):903–7. [PubMed: 8610571]
42. Veillard E, Guggenbuhl P, Morcet N, et al. Prompt regression of paravertebral and epidural abscesses in patients with pyogenic discitis. Sixteen cases evaluated using magnetic resonance imaging. Joint, bone, spine : revue du rhumatisme 2000;67(3):219–27.
43. Kowalski TJ, Layton KF, Berbari EF, et al. Follow-up MR imaging in patients with pyogenic spine infections: lack of correlation with clinical features. AJNR American journal of neuroradiology 2007;28(4):693–9. [PubMed: 17416823]
44. Issa K, Pourtaheri S, Stewart T, et al. Clinical Differences Between Monomicrobial and Polymicrobial Vertebral Osteomyelitis. Orthopedics 2017;40(2):e370–e73. [PubMed: 27841926]
45. Arnold R, Rock C, Croft L, et al. Factors associated with treatment failure in vertebral osteomyelitis requiring spinal instrumentation. Antimicrobial agents and chemotherapy 2014;58(2):880–4. [PubMed: 24277039]
46. Jain NK, Dao K, Ortiz AO. Radiologic evaluation and management of postoperative spine paraspinal fluid collections. Neuroimaging clinics of North America 2014;24(2):375–89. [PubMed: 24792615]
47. Abdul-Jabbar A, Berven SH, Hu SS, et al. Surgical site infections in spine surgery: identification of microbiologic and surgical characteristics in 239 cases. Spine 2013;38(22):E1425–31. [PubMed: 23873240]

48. Gu W, Tu L, Liang Z, et al. Incidence and risk factors for infection in spine surgery: A prospective multicenter study of 1764 instrumented spinal procedures. American journal of infection control 2018;46(1):8–13. [PubMed: 29129272]
49. Van Goethem JW, Parizel PM, van den Hauwe L, et al. The value of MRI in the diagnosis of postoperative spondylodiscitis. Neuroradiology 2000;42(8):580–5. [PubMed: 10997563]
50. McLellan AM, Daniel S, Corcuera-Solano I, et al. Optimized imaging of the postoperative spine. Neuroimaging clinics of North America 2014;24(2):349–64. [PubMed: 24792613]
51. Stecher JM, El-Khoury GY, Hitchon PW. Cervical facet joint septic arthritis: a case report. The Iowa orthopaedic journal 2010;30:182–7. [PubMed: 21045995]
52. Muffoletto AJ, Ketonen LM, Mader JT, et al. Hematogenous pyogenic facet joint infection. Spine 2001;26(14):1570–6. [PubMed: 11462088]
53. Tomoda Y, Kihara Y, Kozuma R, et al. Septic arthritis of the cervical facets: Unusual cause of neck pain. Journal of general and family medicine 2018;19(4):143–44. [PubMed: 29998047]
54. Weingarten TN, Hooten WM, Huntoon MA. Septic facet joint arthritis after a corticosteroid facet injection. Pain medicine 2006;7(1):52–6. [PubMed: 16533197]
55. Tali ET, Oner AY, Koc AM. Pyogenic spinal infections. Neuroimaging clinics of North America 2015;25(2):193–208. [PubMed: 25952173]
56. Egawa Y, Matsumura C, Kawahito T, et al. [A case of the successful treatment of pulmonary artery pseudoaneurysm after PA banding]. [Zasshi] [Journal] Nihon Kyobu Geka Gakkai 1993;41(2): 273–6.
57. Lehman VT, Murthy NS, Diehn FE, et al. The posterior ligamentous complex inflammatory syndrome: spread of fluid and inflammation in the retrodural space of Okada. Clinical radiology 2015;70(5):528–35. [PubMed: 25577652]
58. Murthy NS, Maus TP, Aprill C. The retrodural space of Okada. AJR American journal of roentgenology 2011;196(6):W784–9. [PubMed: 21606270]
59. Doita M, Nishida K, Miyamoto H, et al. Septic arthritis of bilateral lumbar facet joints: report of a case with MRI findings in the early stage. Spine 2003;28(10):E198–202. [PubMed: 12768159]
60. Maus T Imaging the back pain patient. Physical medicine and rehabilitation clinics of North America 2010;21(4):725–66. [PubMed: 20977958]
61. Yachoui R, Han BK, Kolasinski SL. Posterior spondylitis of costovertebral joints in a patient with psoriatic arthritis. Journal of clinical rheumatology : practical reports on rheumatic & musculoskeletal diseases 2012;18(8):450. [PubMed: 23211588]
62. Kim CJ, Song KH, Jeon JH, et al. A comparative study of pyogenic and tuberculous spondylodiscitis. Spine 2010;35(21):E1096–100. [PubMed: 20838270]
63. Dobson J Percivall Pott. Annals of the Royal College of Surgeons of England 1972;50(1):54–65. [PubMed: 4550865]
64. Bell D, Cockshott WP. Tuberculosis of the vertebral pedicles. Radiology 1971;99(1):43–8. [PubMed: 5548686]
65. Tan LA, Kasliwal MK, Nag S, et al. Rapidly progressive quadriparesis heralding disseminated coccidioidomycosis in an immunocompetent patient. Journal of clinical neuroscience : official journal of the Neurosurgical Society of Australasia 2014;21(6):1049–51. [PubMed: 24321458]
66. Williams RL, Fukui MB, Meltzer CC, et al. Fungal spinal osteomyelitis in the immunocompromised patient: MR findings in three cases. AJNR American journal of neuroradiology 1999;20(3):381–5. [PubMed: 10219401]
67. Resorlu H, Sacar S, Inceer BS, et al. Cervical Spondylitis and Epidural Abscess Caused by Brucellosis: a Case Report and Literature Review. Folia medica 2016;58(4):289–92. [PubMed: 28068278]
68. Koubaa M, Maaloul I, Marrakchi C, et al. Spinal brucellosis in South of Tunisia: review of 32 cases. The spine journal : official journal of the North American Spine Society 2014;14(8):1538–44. [PubMed: 24331843]
69. Hong SH, Choi JY, Lee JW, et al. MR imaging assessment of the spine: infection or an imitation? Radiographics : a review publication of the Radiological Society of North America, Inc 2009;29(2):599–612.

70. Caudron A, Grados F, Boubrit Y, et al. Discitis due to Clostridium perfringens. Joint, bone, spine : revue du rhumatisme 2008;75(2):232–4.

71. Albert HB, Lambert P, Rollason J, et al. Does nuclear tissue infected with bacteria following disc herniations lead to Modic changes in the adjacent vertebrae? European spine journal : official publication of the European Spine Society, the European Spinal Deformity Society, and the European Section of the Cervical Spine Research Society 2013;22(4):690–6.

72. Ganko R, Rao PJ, Phan K, et al. Can bacterial infection by low virulent organisms be a plausible cause for symptomatic disc degeneration? A systematic review. Spine 2015;40(10):E587–92. [PubMed: 25955094]

73. Albert HB, Sorensen JS, Christensen BS, et al. Antibiotic treatment in patients with chronic low back pain and vertebral bone edema (Modic type 1 changes): a double-blind randomized clinical controlled trial of efficacy. European spine journal : official publication of the European Spine Society, the European Spinal Deformity Society, and the European Section of the Cervical Spine Research Society 2013;22(4):697–707.

74. Mollerup S, Friis-Nielsen J, Vinner L, et al. Propionibacterium acnes: Disease-Causing Agent or Common Contaminant? Detection in Diverse Patient Samples by Next-Generation Sequencing. Journal of clinical microbiology 2016;54(4):980–7. [PubMed: 26818667]

75. Rigal J, Thelen T, Byrne F, et al. Prospective study using anterior approach did not show association between Modic 1 changes and low grade infection in lumbar spine. European spine journal : official publication of the European Spine Society, the European Spinal Deformity Society, and the European Section of the Cervical Spine Research Society 2016;25(4):1000–5.

76. Georgy M, Stern M, Murphy K. What Is the Role of the Bacterium Propionibacterium acnes in Type 1 Modic Changes? A Review of the Literature. Canadian Association of Radiologists journal = Journal l'Association canadienne des radiologistes 2017;68(4):419–24.

77. Wagner AL, Murtagh FR, Arrington JA, et al. Relationship of Schmorl's nodes to vertebral body endplate fractures and acute endplate disk extrusions. AJNR American journal of neuroradiology 2000;21(2):276–81. [PubMed: 10696008]

78. Stabler A, Bellan M, Weiss M, et al. MR imaging of enhancing intraosseous disk herniation (Schmorl's nodes). AJR American journal of roentgenology 1997;168(4):933–8. [PubMed: 9124143]

79. Hayami N, Hoshino J, Suwabe T, et al. Destructive Spondyloarthropathy in Patients on Long-Term Peritoneal Dialysis or Hemodialysis. Therapeutic apheresis and dialysis : official peer-reviewed journal of the International Society for Apheresis, the Japanese Society for Apheresis, the Japanese Society for Dialysis Therapy 2015;19(4):393–8.

80. Kiss E, Keusch G, Zanetti M, et al. Dialysis-related amyloidosis revisited. AJR American journal of roentgenology 2005;185(6):1460–7. [PubMed: 16303998]

81. Theodorou DJ, Theodorou SJ, Resnick D. Imaging in dialysis spondyloarthropathy. Seminars in dialysis 2002;15(4):290–6. [PubMed: 12191028]

82. Freedman BA, Heller JG. Kummel disease: a not-so-rare complication of osteoporotic vertebral compression fractures. Journal of the American Board of Family Medicine : JABFM 2009;22(1): 75–8. [PubMed: 19124637]

83. McNamara AL, Dickerson EC, Gomez-Hassan DM, et al. Yield of Image-Guided Needle Biopsy for Infectious Discitis: A Systematic Review and Meta-Analysis. AJNR American journal of neuroradiology 2017;38(10):2021–27. [PubMed: 28882866]

84. Kim CJ, Song KH, Park WB, et al. Microbiologically and clinically diagnosed vertebral osteomyelitis: impact of prior antibiotic exposure. Antimicrobial agents and chemotherapy 2012;56(4):2122–4. [PubMed: 22232286]

85. Marschall J, Bhavan KP, Olsen MA, et al. The impact of prebiopsy antibiotics on pathogen recovery in hematogenous vertebral osteomyelitis. Clinical infectious diseases : an official publication of the Infectious Diseases Society of America 2011;52(7):867–72. [PubMed: 21427393]

86. Berbari EF, Kanj SS, Kowalski TJ, et al. Executive Summary: 2015 Infectious Diseases Society of America (IDSA) Clinical Practice Guidelines for the Diagnosis and Treatment of Native Vertebral

Osteomyelitis in Adults. Clinical infectious diseases : an official publication of the Infectious Diseases Society of America 2015;61(6):859–63. [PubMed: 26316526]

87. Michel SC, Pfirrmann CW, Boos N, et al. CT-guided core biopsy of subchondral bone and intervertebral space in suspected spondylodiskitis. AJR American journal of roentgenology 2006;186(4):977–80. [PubMed: 16554566]
88. White LM, Schweitzer ME, Deely DM, et al. Study of osteomyelitis: utility of combined histologic and microbiologic evaluation of percutaneous biopsy samples. Radiology 1995;197(3):840–2. [PubMed: 7480765]

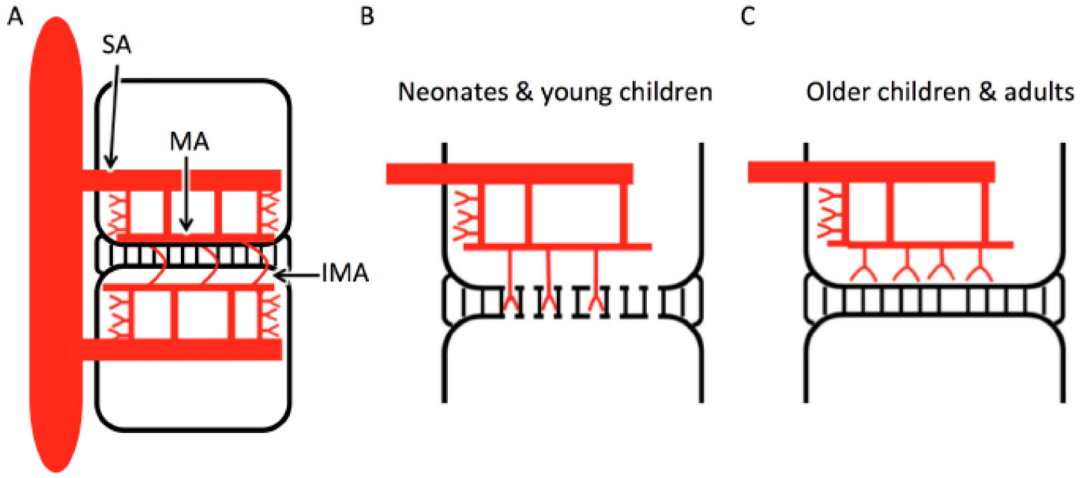

Figure 1.

Hematogenous seeding in discitis-osteomyelitis. A) In adults, segmental arteries (SA) supply each vertebral body and give rise to upper and lower metaphyseal anastomosing arteries (MA) which traverse horizontally adjacent to each endplate. Communication between adjacent vertebral MAs via intermetaphyseal anastomosing arteries (IMA) allows for infectious spread across the disc space. B) Neonates and young children have rich arterial supply to the disc via endplate perforations. C) This direct vascular supply to the disc is not found in older children and adults.

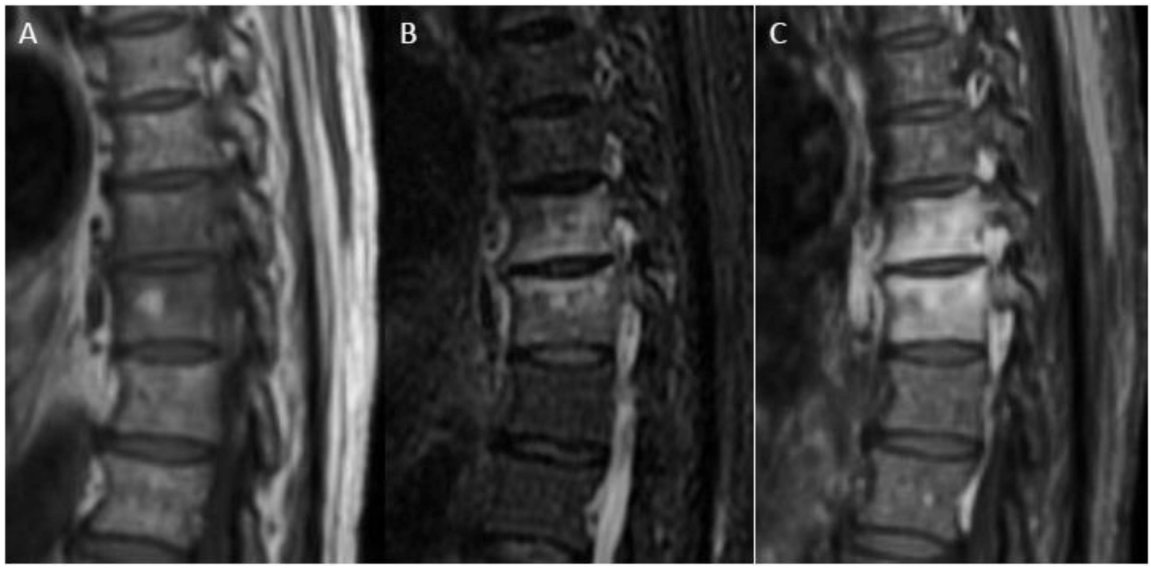

Figure 2.

MRI in early discitis-osteomyelitis (DOM). Coned-in sagittal T1w (A), T2w FS (B), and T1-post contrast FS (C) images of the mid thoracic spine reveal abnormal fluid signal and enhancement involving the T8 and T9 vertebral bodies. During this early stage of pyogenic DOM, there is relative sparing of the T8–9 disc and no bony erosion or significant extra-spinal spread of infection.

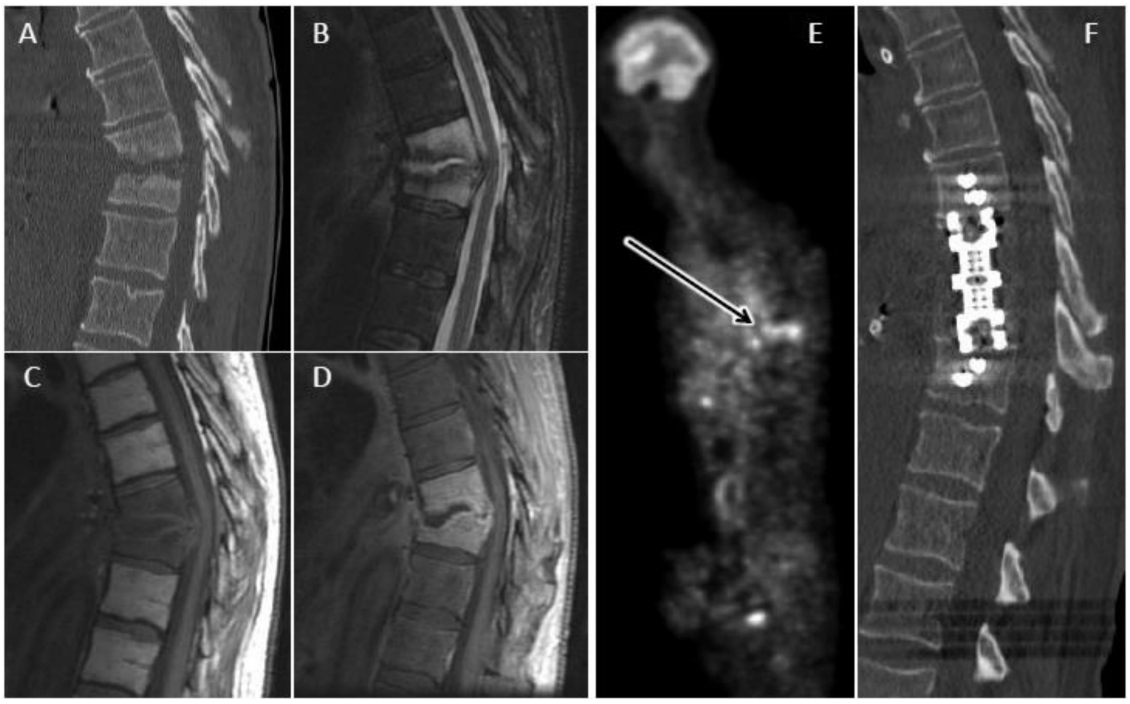

Figure 3.

Advanced DOM. Sagittal CT (A) of the thoracic spine reveals extensive endplate and vertebral body erosion centered about an eroded T9-T10 disc space with associated kyphotic deformity in this 64 year old male with advanced pyogenic DOM. Sagittal T2 FS (B), T1 (C), and T1 post FS (D) images through the same level confirm abnormal fluid signal and enhancement throughout the involved vertebral levels. Non-enhancing fluid in the eroded disc space is characteristic of advanced DOM. E) Whole body FDG-PET reveals increased radionuclide uptake at the level of infection (arrow). F) Post-operative CT reveals restoration of spinal alignment following T9-T10 corpectomy and intervertebral cage placement.

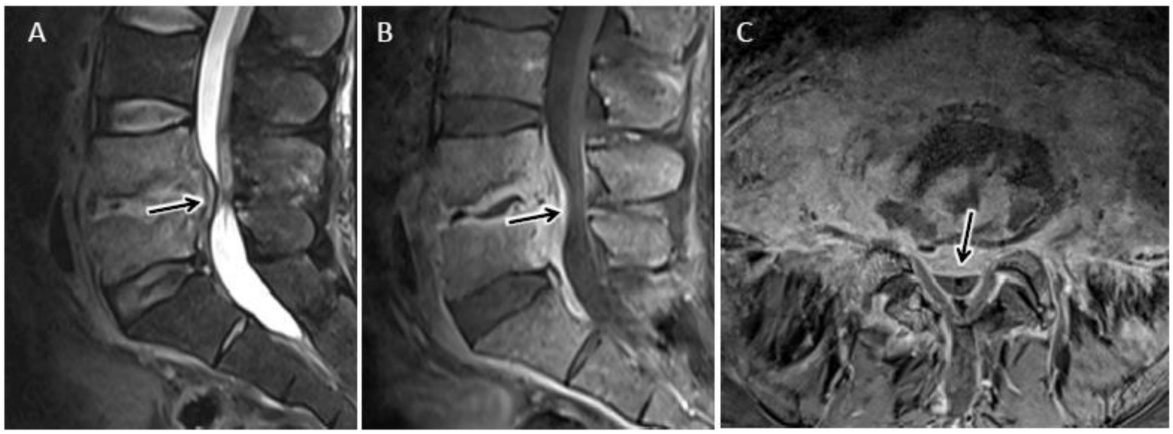

Figure 4.

Advanced lumbar DOM with extension beyond the discovertebral complex. Sagittal T2 (A), sagittal (B), and axial (C) T1 post contrast MR images coned in to the lower lumbar spine show characteristic MR features of L4-L5 DOM. In addition, there is prominent ventral epidural extension of phlegmonous infection (arrow in A-C) contributing to spinal canal stenosis. Axial T1-post contrast image (C) best demonstrates the extensive ventral and anterolateral paraspinous extension of infection without drainable fluid collection.

Figure 5.

Advanced cervical DOM with extension beyond the discovertebral complex. Sagittal T2 (A), sagittal (B), and axial (C) T1 post contrast MR images coned in to the mid cervical spine show characteristic MR features of C5-C6 DOM with advanced disc and endplate destruction. In addition, there is prominent ventral epidural extension of phlegmonous infection (arrow in A-C) contributing to spinal canal stenosis and spinal cord compression. C) Axial T1-post contrast image best demonstrates the right more than left ventral and lateral paraspinous extension of infection without drainable fluid collection.

Figure 6.

Cervical epidural abscess with reduced diffusion. 48 year-old man with history significant for intravenous drug abuse presents with progressive weakness and quadriplegia. Sagittal T2-w (A) and sagittal (B) and axial (C) T1-w post contrast MR images of the cervical spine reveal a longitudinally extensive ventral epidural fluid collection with peripheral enhancement and spinal cord compression. Sagittal DWI (D) image and corresponding ADC map (E) through the same level demonstrate abnormal reduced diffusion associated with this epidural abscess.

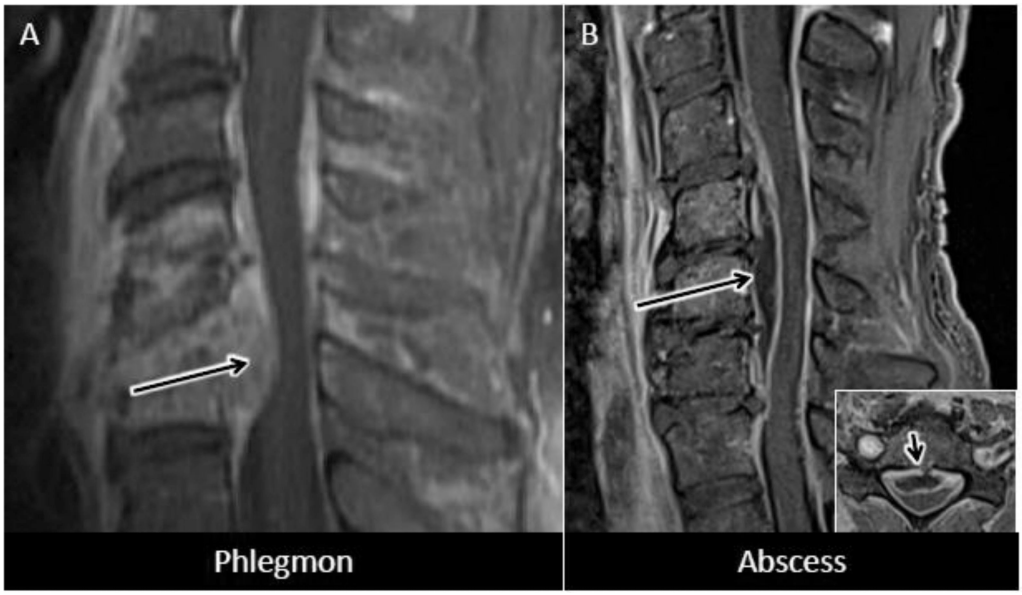

Figure 7.

Epidural phlegmon versus epidural abscess. A) Sagittal T1 post-contrast MR image shows destructive changes of C5-C6 DOM with prominent solidly enhancing ventral epidural phlegmon. B) More subtle C5–6 DOM with adjacent peripherally enhancing fluid collection in the ventral epidural space spanning the C4–5 through C6–7 levels (long arrow) consistent with epidural abscess. Right lower corner inset in 'B' shows axial T1-post contrast MR at the C6 level with well-circumscribed ventral epidural abscess (short arrow) severely narrowing the spinal canal.

Figure 8.

DOM with epidural phlegmon and spinal cord compression. Sagittal CT (A), T1 post contrast (B), and T2 (C) MR images centered at the T9 vertebral level in a 25 year-old female with paraplegia, back pain, and methicillin sensitive *S. aureus* (MSSA) bacteremia shows advanced destructive changes of the T9 vertebral body with focal kyphosis and prominent epidural phlegmon contributing to spinal cord compression. Arrows in 'C' show inferior extent of central spinal cord T2 hyperintensity related to cord compression.

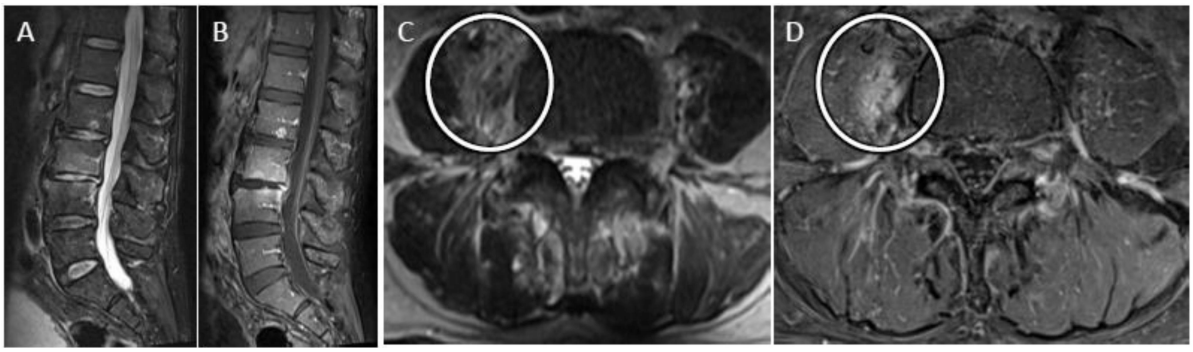

Figure 9.

Psoas sign. Sagittal T2 FS (A) and T1 post FS (B) images of the lumbar spine showing abnormal fluid signal and enhancement of the L3 and L4 vertebral bodies as may be seen with DOM as well as with Modic type 1 fibrovascular reactive marrow edema. C) Axial T2 image at the L3 vertebral level shows asymmetric right psoas muscle T2-hyperintense edema consistent with the ‘psoas’ sign, favoring a diagnosis of early DOM. D) Axial T1 post FS image at same level as ‘C’ reveals abnormal enhancement corresponding to myositic edema seen on T2.

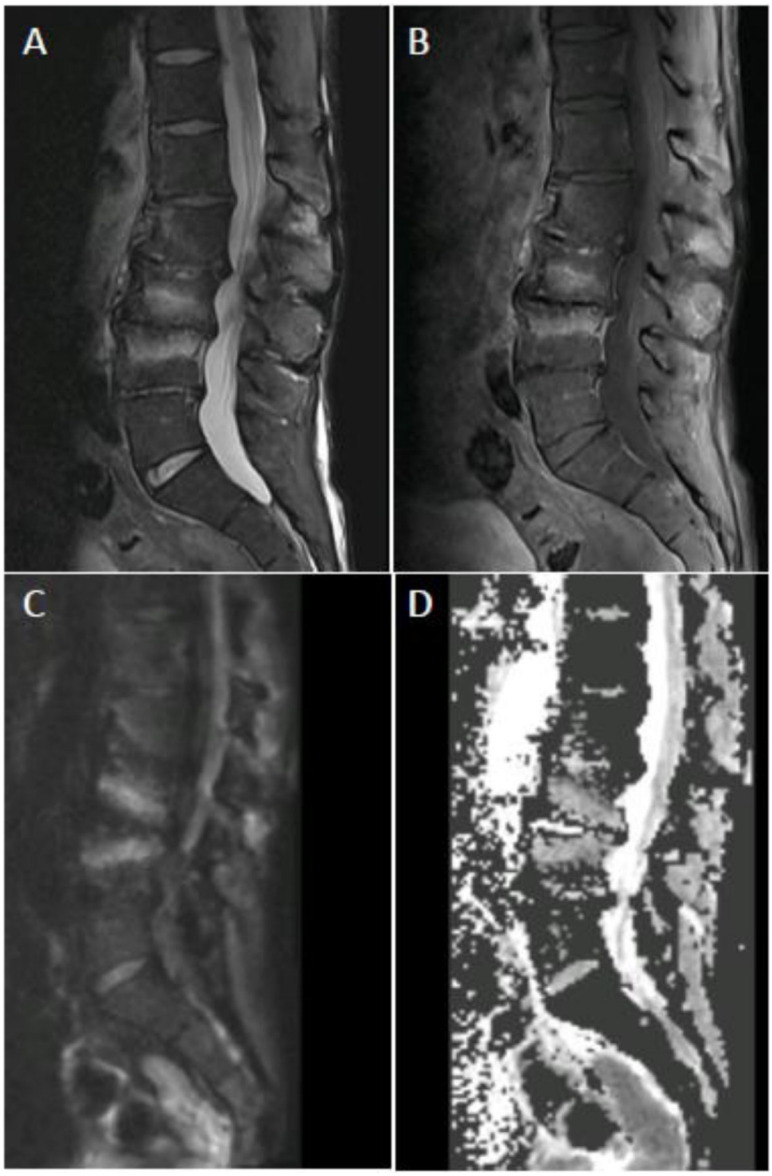

Figure 10.

Claw sign. Sagittal T2 FS (A) and T1 post FS (B) MR images of the lumbar spine showing abnormal fluid signal and enhancement of the L3 and L4 vertebral bodies as may be seen with DOM as well as with Modic type 1 fibrovascular reactive marrow edema. C) Sagittal diffusion weighted image shows well circumscribed, paired, leading edge DWI hyperintense bands emanating from the L3-L4 disc consistent with the ‘claw’ sign favoring a diagnosis of Modic type 1 reactive edema. D) Sagittal ADC map shows corresponding elevated ADC signal relative to normal intervertebral disc consistent with T2-shine-through.

Figure 11.

Diffusion imaging for DOM. A) Sagittal T1 post contrast image coned in to the L4-L5 level shows abnormal L4 and L5 vertebral body enhancement with endplate and disc erosion and ventral epidural phlegmon. B) Sagittal DWI reveals relatively uniform hyperintense signal throughout the involved disc and vertebral bodies with absence of the ‘claw’ sign, consistent with DOM. C) Sagittal ADC map with relative isointense to mildly hypointnese signal relate to normal intervertebral disc in areas of DWI hyperintensity.

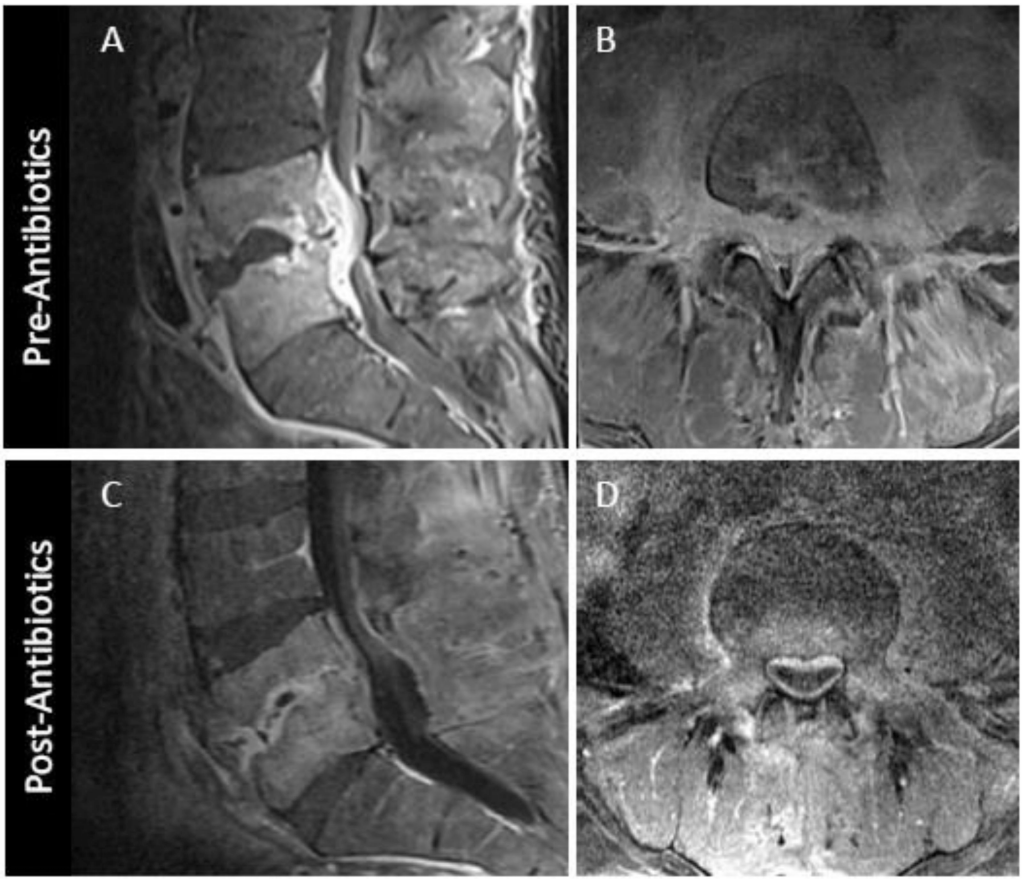

Figure 12.

MRI appearance of DOM before and 8 weeks after successful antibiotic treatment. Sagittal (A) and axial (B) T1 post contrast images coned in to the L4-L5 level show advanced DOM at this level with liquification of the L4-L5 disc, endplate erosion, and prominent ventral epidural and paraspinous spread of infection. Following 8 weeks of antibiotic therapy, axial T1 post contrast MR image (C) shows some progressive vertebral body erosion and height loss at L4-L5 with persistent abnormal marrow enhancement. Axial T1 postcontrast images (D) however, reveals significant decrease in epidural and paraspinous phlegmon, a more reliable indicator of interval response to therapy.

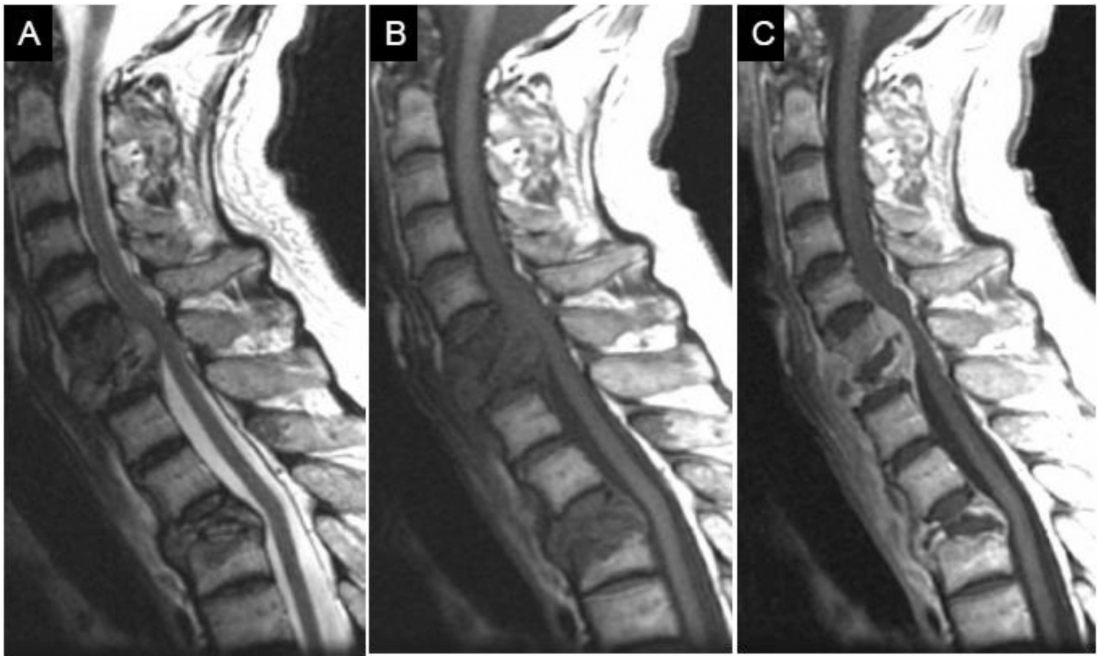

Figure 13.

Polymicrobial spine infection. 56 year-old man with back pain. Sagittal T2 (A), T1 (B) and post-gadolinium T1 (C) MR images of the cervical and upper thoracic spine demonstrate erosion and loss of height of the C6, C7 and T3 vertebrae. There is abnormal high T2, low T1 signal and enhancement at the levels of spinal infection. There is cord compression at C6–7 and associated kyphosis at T3, consistent with Pott's spine. Surgical biopsy cultures were positive for both TB and corynebacterium species.

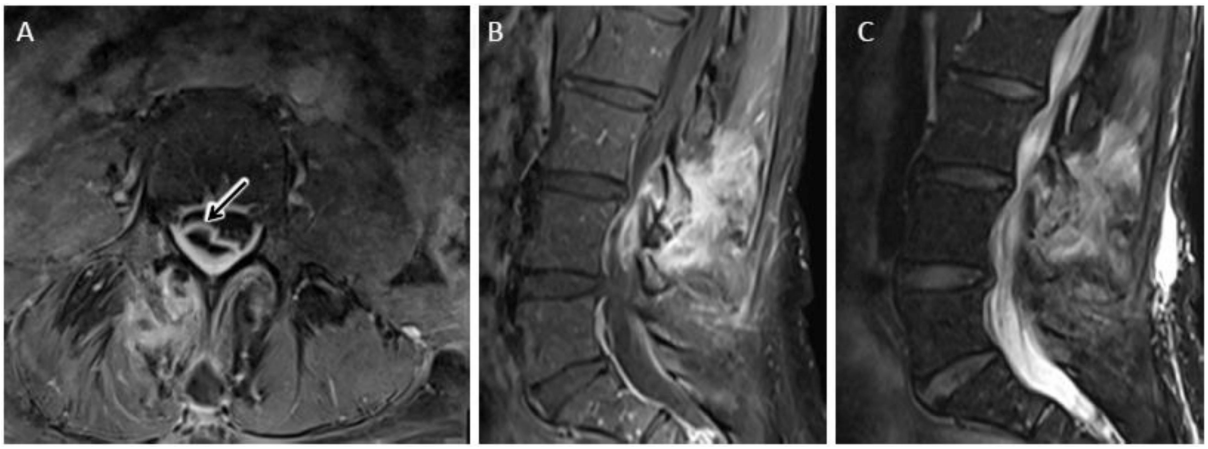

Figure 14.

Septic facet arthropathy with epidural abscess. Axial (A) and sagittal (B) T1 post contrast MR images show avid bone, synovial and peri-articular enhancement of the right L3-L4 facet joint with corresponding T2 hyperintense edema (C). Arrow in 'A' identifies associated right dorsolateral epidural abscess related to septic facet arthritis.

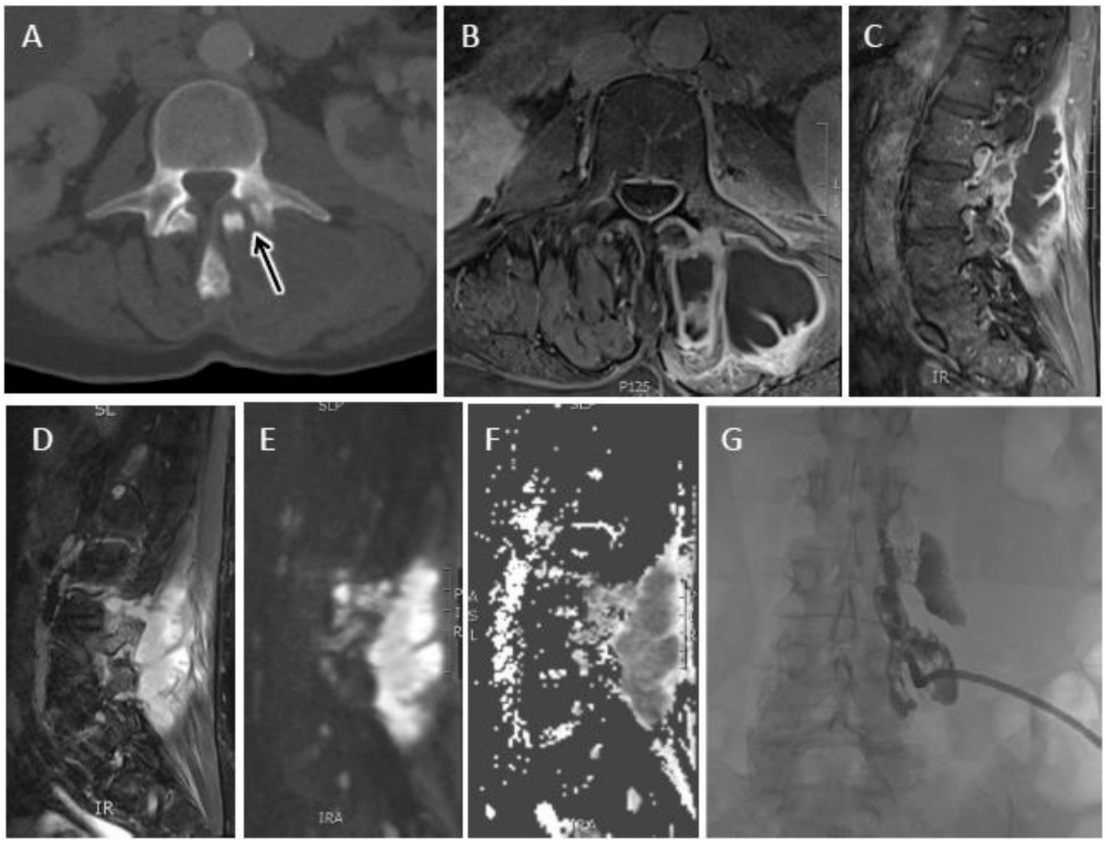

Figure 15.

Septic facet arthropathy with large paraspinal abscess. Axial CT image shows abnormal erosion and widening of the left L3-L4 facet joint (arrow). Axial (B) and sagittal (C) T1 post contrast and T2 (D) images show a complex peripherally enhancing abscess involving the adjacent left multifidis and erector spinae muscles. Sagittal DWI (E) and ADC map (F) display corresponding central reduced diffusion in cystic components consistent with purulent contents. Percutaneous drainage with a pigtail catheter was performed. G) Coronal fluoroscopic image of the lumbar spine shows contrast delineating the complex paraspinous abscess.

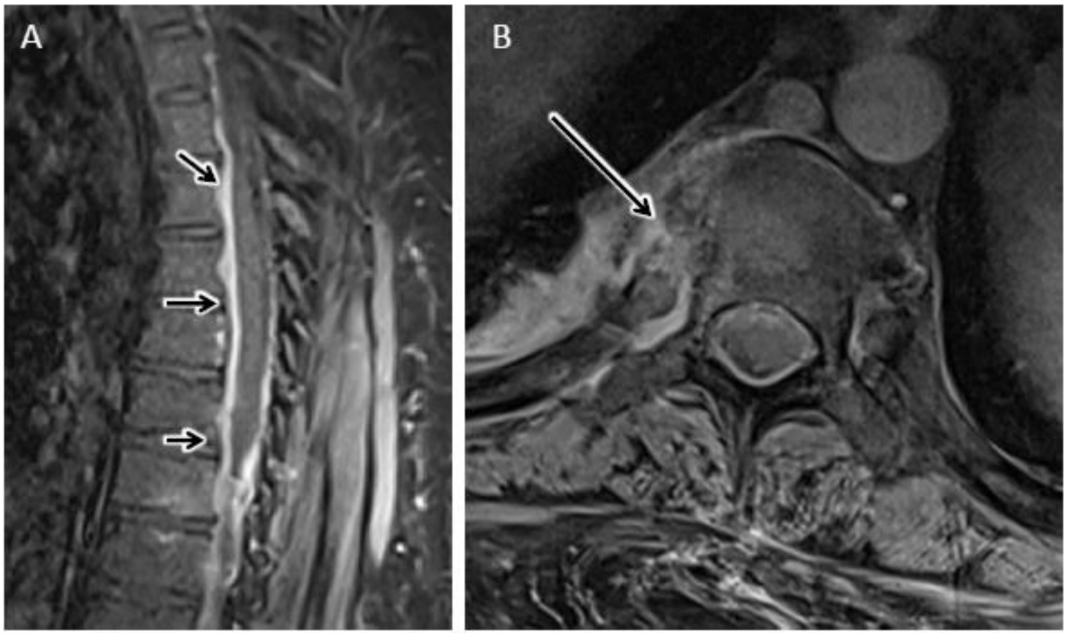

Figure 16.

Septic costo-vertebral joint in a 49 year-old male with elevated CRP and back pain. A) Sagittal T1 post contrast FS MR image of the thoracic spine shows longitudinally extensive ventral-predominant epidural thickening and hyperenhancement (short arrows) without evidence for DOM at any thoracic level. B) Axial T1 post contrast FS MR image at the T7 levels shows abnormal bone and peri-articular enhancement centered about the right 7th costovertebral joint, consistent with septic arthropathy.

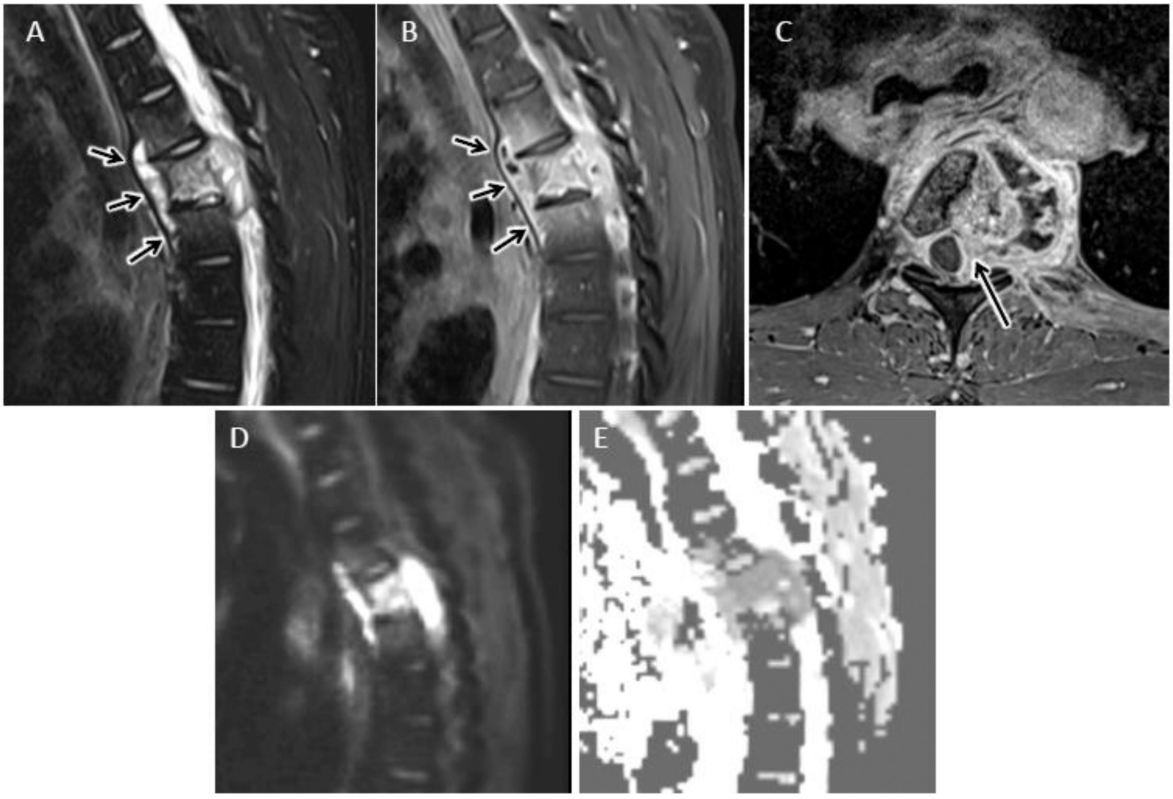

Figure 17.

Tuberculous spondylitis (TS) in a 31 year old male from central Africa presenting with several month history of cough, fever, night sweats, and 25 lb weight loss. Sagittal T2 FS (A) and T1 post FS (B) MR images reveal abnormal T2 hyperintensity and enhancement centered at T5 with prominent anterior subligamentous spread of infection (arrows). Note relative sparing of the T4–5 and T5–6 intervertebral discs. C) Axial T1 post contrast MR image shows T5 osteomyelitis with left more than right epidural extension (arrow) and irregular left paraspinous abscess. Sagittal DWI (D) and ADC map (E) reveals confluent reduced diffusion in regions of solidly enhancing infection. Percutanous biopsy confirmed the suspected diagnosis of TS.

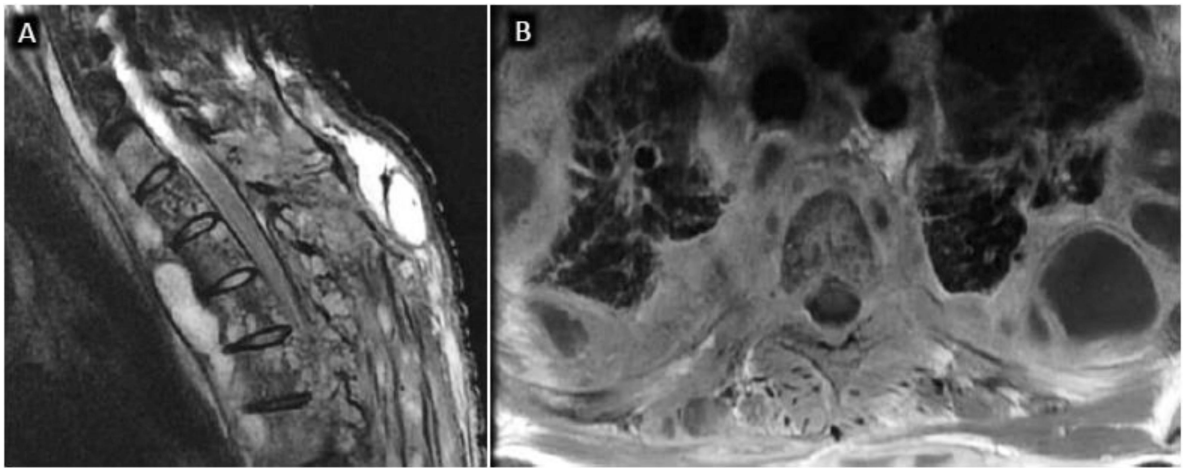

Figure 18.

Disseminated fungal spondylitis in a 28 year old immunocompromised female with chronic granulomatous disease. Sagittal T2 (A) and axial T1 post contrast (B) MR images shows diffuse osteomyelitis of the visualized spine with extensive extranspinal phlegmon and multi-loculated abscesses. Biopsy confirmed disseminated invasive aspergillosis.

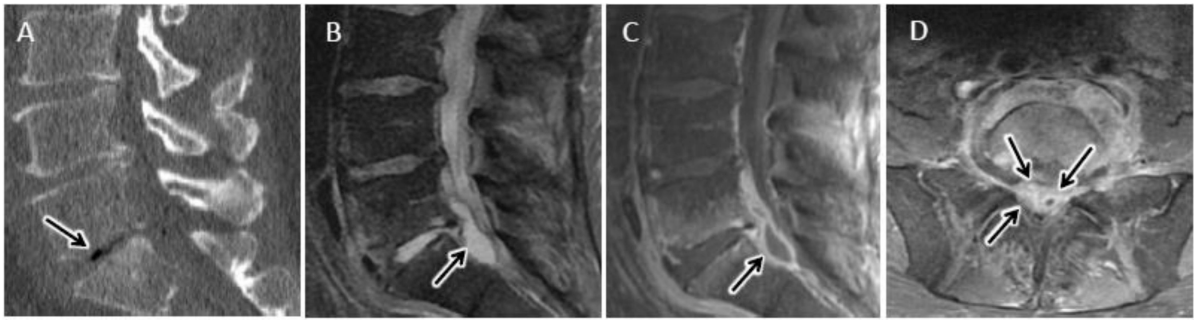

Figure 19.

Degenerative vacuum phenomenon with coexistent acute pyogenic DOM. A) Sagittal CT image coned in to the lower lumbar spine from a 48 year old man presenting with 1 month of progressive low back pain shows advanced disc height loss and gas within the L5-S1 disc consistent with degenerative vacuum phenomenon (*arrow in A*). Sagittal T2-w (B) and sagittal (C) and axial (D) T1-w post contrast FS images from lumbar spine performed on the same day as CT shows findings consistent with acute L5-S1 DOM with prominent ventral epidural abscess (*arrow in B and C*) and epidural phlegmon centered at the L5-S1 level (*arrows in D*).

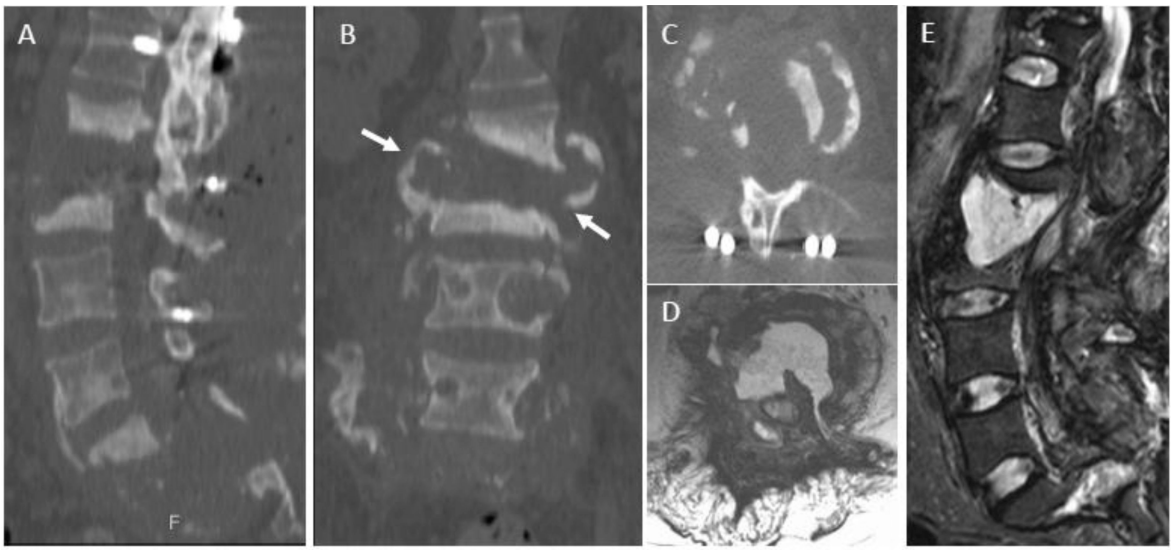

Figure 20.

Spinal neuroarthropathy (SNA) as a mimic of discitis-osteomyelitis in a 58-year-old male with multilevel destructive SNA 7 years after traumatic paraplegia, most pronounced at L2–L3 and S1-S2. CT scan with sagittal (A), coronal (B), and axial (C) plane images and MRI with axial (D) and sagittal (E) T2w images show complete destruction of the discovertebral unit at L2–3 with osseous debris extending beyond the vertebral body (*arrows in B*) as well as presence of an intervertebral collection. Extensive destruction of the sacrum is also seen.

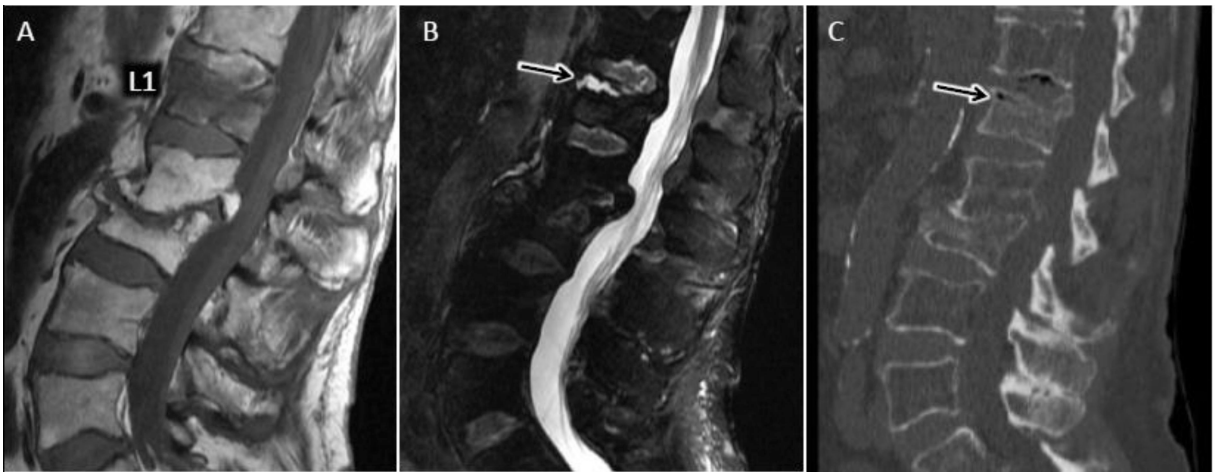

Figure 21.

Avascular necrosis (AVN) of vertebral body after osteoporotic compression (Kummel disease) as a mimic of DOM. Sagittal T1 (A) and T2 FS (B) MR images show T1 hypointense signal throughout the L1 vertebral body with more focal T2 hyperintense fluid signal cleft (arrow), characteristic of transudative fluid collection along widened intravertebral pseudoarthrosis associated with AVN. C) Sagittal CT with hypodense air (arrow) along pseudoarthrosis of AVN fracture related to vacuum phenomenon (air cleft sign). Chronic healed L2 and L3 osteoporotic fractures are also present.

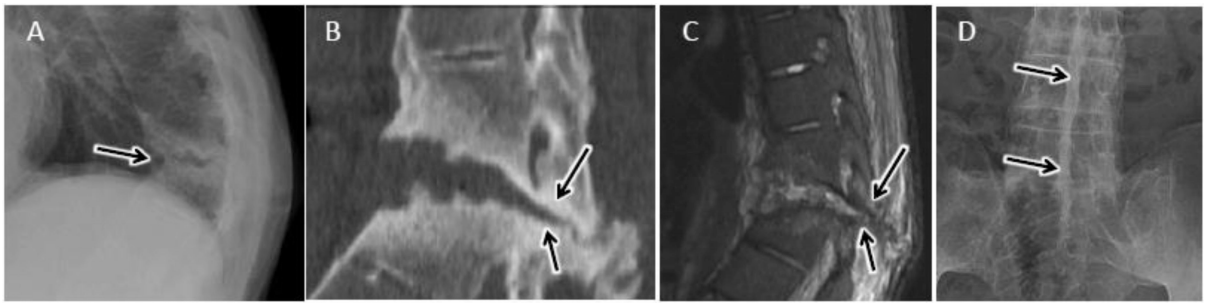

Figure 22.

Post-traumatic pseudoarthrosis in ankylosing spondylitis as a mimic of discitisostemyelitis in 47 year old male with progressive LBP and remote fall 4–5 years prior and history of positive PPD. A) Lateral radiograph of the thoracic spine shows focal kyphotic deformity centered at T10-T11 with discovertebral destruction and subchondral sclerosis (arrow). Sagittal coned-in CT (B) and sagittal T2-w MR image (C) at the T10-T11 level again demonstrates discovertebral destruction at this level with focal kyphosis and linear fracture line/pseudoarthrosis extending across the posterior elements (arrow in B and C). Minimal reactive marrow edema along the pseudoarthrosis is present. Squaring of the vertebral bodes with flowing syndesmophites are noted at levels above and below the pseudoarthrosis. D) AP radiograph of the lumbar spine shows linear fusion of the spinous processes (dagger sign), as seen with ankylosing spondylitis.

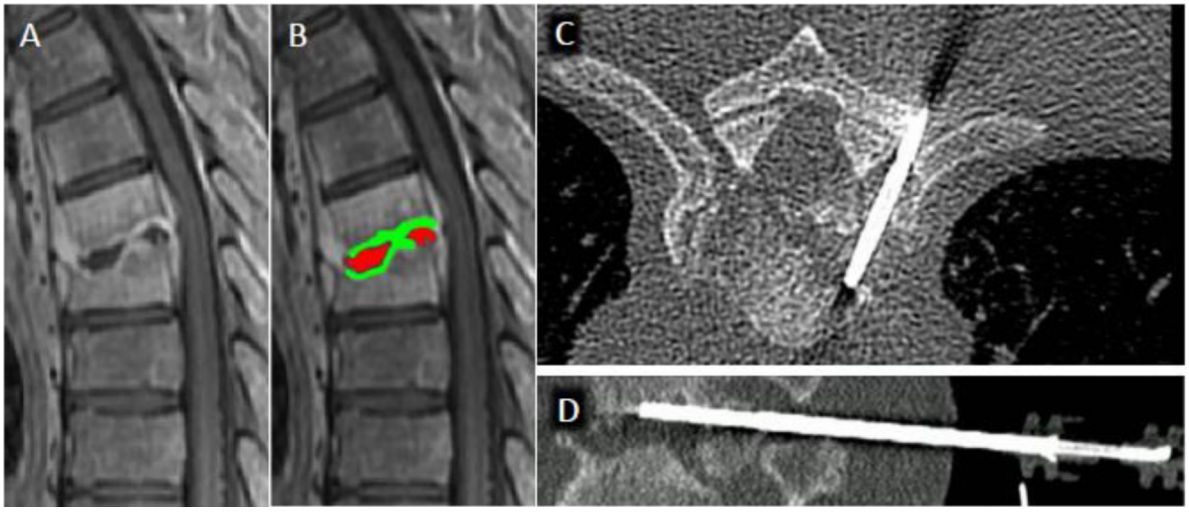

Figure 23.

CT-guided percutaneous biopsy for discitis-osteomyelitis (DOM). A) Sagittal T1 post contrast MR image centered at the mid-thoracic spine shows abnormal T6 and T7 vertebral body enhancement with endplate erosion and liquefaction of the T6-T7 disc space. B) Sampling of the non-enhancing purulent disc material (delineated in red) tends to yield sterile specimens, therefore inclusion of the adjacent enhancing vertebral endplate and subchondral bone (delineated in green) tends to produce higher yields. Axial (C) and sagittal (D) CT images from biopsy procedures shows positioning of the core biopsy needle to include both disc and superior endplate/subchondral bone.